Ultrasonics 52 (2012) 33–38

Contents lists available at ScienceDirect

Ultrasonics

journal homepage: www.elsevier.com/locate/ultras

Propagation behaviors of thickness–twist modes in an inhomogeneous piezoelectric plate with two imperfectly bonded interfaces

Feng Jin *, Peng Li

MOE Key Laboratory for Strength and Vibration, School of Aerospace, Xi'an Jiaotong University, Xi'an 710049, PR China

ARTICLE INFO

Article history:
Received 17 February 2011
Accepted 9 June 2011
Available online 21 June 2011

Keywords:
Thickness–twist mode
Mechanical imperfection
Electrical imperfection
Spring-type relation
Shear-lag model

ABSTRACT

The thickness–twist modes in an inhomogeneous piezoelectric plate with two imperfectly bonded interfaces are analyzed, and an exact solution is obtained according to the spring-type relation from the equations of the linear theory of piezoelectricity. The frequency shift, the displacement and the stress components are all obtained and plotted. Both theoretical analysis and numerical examples show that the effect of mechanical imperfection is more evident than that of the electrical imperfection on the thickness–twist modes. Results show that the displacement and the stress components all change obviously due to the imperfectly bonded interfaces. The relationship between the frequency shift $\Delta\omega$ and the non-dimensional number γ that is related to the imperfect interfaces is linear, which can be used to provide the foundation for a new experimental procedure for measuring the level of the interface bonding.

1. Introduction

Piezoelectric materials can be made into various functional devices, such as sensors, actuators, filters and delay lines, which are widely used in electronic technology, mechanical engineering, medical appliance and other modern industrial fields [1]. Owing to wide application, the mechanism study of propagation of waves in piezoelectric structures and devices has drawn increasing attention of researchers in recent years [2–4]. Thickness–twist vibration modes (anti-plane or shear horizontal modes) of crystal plates are often used as the operating modes for resonators and acoustic wave sensors [5,6]. When the sixfold axis of a 6 mm crystal is parallel to the major surface of a plate, thickness–twist waves can propagate not only in a homogeneous piezoelectric plate [7,8], but in an inhomogeneous piezoelectric plate as well [9–11].

In principle, the mechanical and the electrical behaviors in piezoelectric materials should satisfy the kinetic equations and Maxwell equations. Along this approach, the shear horizontal waves in two inhomogeneous media [12,13] and in functionally graded piezoelectric layered structures [14,15] have been respectively investigated. Meanwhile, due to the brittleness nature of piezoelectric ceramics and the possible defects of impurity, cavities and micro-cracks, failures of devices take place easily under mechanical and/or electrical loadings. In order to overcome above-mentioned disadvantages, the shear horizontal waves in a pre-stressed layered piezoelectric structure have been considered [16–18]. Besides, SAW devices loaded with viscous liquid have also been taken into account [19,20].

However, most of the work is on the perfectly bonding interface between the two portions, i.e. the displacement and the tractions are continuous [12–20]. It has been recently pointed out that imperfectly bonding sometimes exists in devices and little is known about its effects [21], e.g., the aging of the glue which is applied at an interface, the defection of fabrication and corrosion of the materials, etc. In the simplest description of the mechanical behavior of an imperfect interface, the interface can be treated as a layer that geometrically has a zero thickness but still possesses elasticity and interface elastic strain energy, e.g., the shear-lag model in which the tangential displacement at an interface is allowed to be different from both sides of the interface in order to accounting for the deformation of the interface layer [22–25].

In this paper, we investigate the effect of the imperfectly bonded interfaces in an inhomogeneous piezoelectric plate in which the central portion is different from the rest portions using a spring-type relation [26], which is different from the shear-lag model [22–25]. Different from the previous work, the mechanical imperfection and the electrical imperfection are all taken into account. Since the material tensors of crystals of 6 mm symmetry have the same structures as polarized ceramics, our analysis is also valid for 6 mm piezoelectric crystals. This includes widely used materials like ZnO and AlN.

2. Governing equations and boundary conditions

Consider an inhomogeneous piezoelectric plate of 6 mm crystals or polarized ceramics with the depth of $2h$, as shown in Fig. 1. The ceramic material is poled in the x_3 direction determined

* Corresponding author. Fax: +86 29 83237910.
E-mail address: jinfengzhao@263.net (F. Jin).

0041-624X/$ - see front matter © 2011 Elsevier B.V. All rights reserved.
doi:10.1016/j.ultras.2011.06.007

by the right-hand rule from the x_1 and x_2 axes. The central portion $x_1 < |a|$ is made of one piezoelectric material, and the outer portions $x_1 > |a|$ are made of another one. We consider the imperfect boundary conditions at $x_1 = |a|$. The plate is unelectroded, and the surfaces are traction-free at $x_2 = \pm h$.

2.1. The governing equations

The thickness–twist mode of the central portion ($x_1 < |a|$) can be represented by displacement components u and electrical potential function φ as follows:

$$u_1 = 0, \quad u_2 = 0, \quad u_3 = u(x_1, x_2, t), \quad \varphi = \varphi(x_1, x_2, t) \tag{1}$$

A function ψ can be introduced through $\varphi = \psi + eu/\varepsilon$ [9–11], and the governing equations of thickness–twist mode can be obtained:

$$\bar{c}\nabla^2 u = \rho\ddot{u}, \quad \nabla^2\psi = 0 \tag{2}$$

where $\nabla^2 = \partial^2/\partial x_1^2 + \partial^2/\partial x_2^2$ is the Laplace operator, ρ is the mass density, $c_{44} = c$, $e_{15} = e$ and $\varepsilon_{11} = \varepsilon$ are the elastic, the piezoelectric and the permittivity coefficients, respectively. The relative elastic constant is $\bar{c} = c + e^2/\varepsilon$. The nontrivial stress and electric displacement components are

$$\begin{aligned} &T_{23} = \bar{c}u_{,2} + e\psi_{,2}, \quad T_{13} = \bar{c}u_{,1} + e\psi_{,1} \\ &D_2 = -\varepsilon\psi_{,2}, \quad D_1 = -\varepsilon\psi_{,1} \end{aligned} \tag{3}$$

where an index after a comma denotes partial differentiation with respect to the coordinate.

Similarly, for the outer regions ($x_1 > |a|$) of the plate, the governing equations are

$$\bar{c}'\nabla^2 u' = \rho'\ddot{u}, \quad \nabla^2\psi' = 0 \tag{4}$$

The nontrivial stress and electric displacement components are

$$\begin{aligned} &T'_{23} = \bar{c}'u'_{,2} + e'\psi'_{,2}, T'_{13} = \bar{c}'u'_{,1} + e'\psi'_{,1} \\ &D'_2 = -\varepsilon'\psi'_{,2}, D'_1 = -\varepsilon'\psi'_{,1} \end{aligned} \tag{5}$$

2.2. The boundary conditions

For the unelectroded and traction-free surfaces, $T_{23} = 0$, $T'_{23} = 0$ and $D_2 = 0$, $D'_2 = 0$ at $x_2 = \pm h$, which are equal to

$$x_2 = \pm h : u_{,2} = 0, \quad u'_{,2} = 0, \quad \psi_{,2} = 0, \quad \psi'_{,2} = 0 \tag{6}$$

For the imperfectly bonded interfaces at $x_1 = \pm a$, we adopt the spring-type relation [8], which requires

$$x_1 = \pm a : \begin{cases} T_{13} = T'_{13} = K(u' - u) \\ D_1 = D'_1 = \Gamma(\varphi' - \varphi) \end{cases} \tag{7}$$

where K (N/m^3) is the effective interface elastic stiffness parameter and Γ (C/V m^2) is the electrical imperfection parameter, which simultaneously describe how well the two materials are bonded.

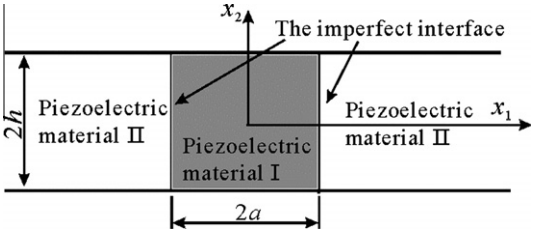

Fig. 1. An inhomogeneous transversely piezoelectric plate that the central portion is different from the rest portions with imperfectly bonded interfaces.

When $K = 0$ and $\Gamma = 0$, the three portions lose their mechanical and electrical interaction. When $K = \infty$ and $\Gamma \neq \infty$, we consider the electrical imperfection only. The circumstance of $\Gamma = \infty$ and $K \neq \infty$ is the only consideration of the mechanical imperfection, which is the same as the shear-lag model [22–25]. The case of $K = \infty$ and $\Gamma = \infty$ is for the perfect interface with continuous displacement and electrical function across the interface.

We assume the two interfaces at $x_1 = \pm a$ have the same characteristics, i.e., they have the same effective interface elastic stiffness K and the same electrical imperfection parameter Γ simultaneously. As we know, this is impossible in practice, but it is helpful to investigate and understand the effect of the imperfect interfaces on the characteristics of the thickness–twist mode waves. Besides, the displacement and the electric potential are finite, which requires

$$|x_1| \to \infty : u' \to 0, \quad \varphi' \to 0 \tag{8}$$

3. Propagating wave solutions

It can be verified that solutions to Eqs. (2) and (4) can be classified into waves symmetric and anti-symmetric in the x_1 direction [5,7,8]. Here we only investigate the waves which are symmetric in the x_1 direction. So for the central portion, we have [9–11]

$$\begin{cases} u = A_1\cos(\xi_1 x_1)\cos(\xi_2 x_2)\exp(i\omega t) \\ \psi = B_1\cosh(\xi_2 x_1)\cos(\xi_2 x_2)\exp(i\omega t) \end{cases} \tag{9}$$

where A_1 and B_1 are undetermined constants, ξ_1 and ξ_2 are wave numbers in the x_1 and x_2 directions, $\xi_2 = \frac{m\pi}{2h}(m = 0, 2, 4, \ldots)$, ω is the wave frequency and $i^2 = -1$. In particular, $m = 0$ is called face-shear mode, which will not be considered in the following.

Eq. (9) has satisfied with Eq. (6) and the second equation in Eq. (2). Inserting Eq. (9) into the first equation in Eq. (2), we have

$$\xi_1 = \sqrt{\frac{\rho\omega^2}{\bar{c}} - \xi_2^2} = \sqrt{\frac{\rho}{\bar{c}}}\sqrt{\omega^2 - \left(\frac{m\pi}{2h}\right)^2\frac{\bar{c}}{\rho}} = \frac{1}{v_r}\sqrt{\omega^2 - \omega_m^2} \tag{10}$$

where $v_T = \sqrt{\bar{c}/\rho}$ is the bulk shear wave velocity of the piezoelectric material occupying $x_1 < |a|$ and $\omega_m = \left(\frac{m\pi}{2h}\right)v_T$ is the corresponding cut-off frequency of thickness–twist waves.

Similarly, for the modes of the outer portions [9–11]

$$\begin{aligned} u' &= \begin{cases} A'_1\exp\left[-\xi'_1(x_1 - a)\right]\cos(\xi_2 x_2)\exp(i\omega t), & x_1 > a \\ A'_1\exp\left[\xi'_1(x_1 + a)\right]\cos(\xi_2 x_2)\exp(i\omega t), & x_1 < -a \end{cases} \\ \psi' &= \begin{cases} B'_1\exp\left[-\xi_2(x_1 - a)\right]\cos(\xi_2 x_2)\exp(i\omega t), & x_1 > a \\ B'_1\exp[\xi_2(x_1 + a)]\cos(\xi_2 x_2)\exp(i\omega t), & x_1 < -a \end{cases} \end{aligned} \tag{11}$$

where A'_1 and B'_1 are undetermined constants, ξ'_1 is the wave number in the x_1 direction, which satisfied

$$\xi'_1 = \sqrt{\xi_2^2 - \frac{\rho'\omega^2}{\bar{c}'}} = \frac{1}{v'_T}\sqrt{\omega'^2_m - \omega^2} \tag{12}$$

Similarly, $v'_T = \sqrt{\bar{c}'/\rho'}$ is the bulk shear wave velocity of the outer piezoelectric material and $\omega'_m = \left(\frac{m\pi}{2h}\right)^2 v'_T$ is the corresponding cut-off frequency.

Substituting Eq. (9) into Eq. (3) and inserting Eq. (11) into Eq. (5) respectively, T_{13}, D_1, T'_{13} and D'_1 can be obtained. According to the boundary conditions Eq. (7), we can get

$$\begin{cases} \bar{c}'A'_1\xi'_1 - e'B'_1\xi_2 = K\left[A'_1 - A_1\cos(\xi_1 a)\right] \\ -\bar{c}A_1\xi_1\sin(\xi_1 a) + eB_1\xi_2\sinh(\xi_2 a) = -\bar{c}'A'_1\xi'_1 - e'B'_1\xi_2 \\ \varepsilon'B'_1\xi_2 = \Gamma\left[B'_1 + \frac{e'}{\varepsilon'}A'_1 - B_1\cosh(\xi_2 a) - \frac{e}{\varepsilon}A_1\cos(\xi_1 a)\right] \\ -\varepsilon B_1\xi_2\sinh(\xi_2 a) = \varepsilon'B'_1\xi_2 \end{cases} \tag{13}$$

Eq. (13) is a four linear, homogeneous equation for A_1, B_1, A_1' and B_1'. For nontrivial solutions, the determinant of the coefficient matrix has to vanish, which yields the frequency equation

$$M = M_{\text{perfect}} + M_K + M_\Gamma + M_{K\Gamma} = 0 \tag{14}$$

where

$$\begin{aligned} M_{\text{perfect}} &= [\bar{c}'\xi_1' - \bar{c}\xi_1 \tan(\xi_1 a)][\varepsilon' + \varepsilon \tanh(\xi_2 a)] \\ &\quad - \xi_2 \varepsilon \varepsilon^2 \left(\frac{e}{\varepsilon} - \frac{e'}{\varepsilon'}\right)^2 \tanh(\xi_2 a), \\ M_k &= -\frac{1}{K}\left\{\bar{c}\xi_1 \bar{c}'\xi_1' \tan(\xi_1 a)[\varepsilon' + \varepsilon \tanh(\xi_2 a)] \right. \\ &\quad \left. + \varepsilon\varepsilon'\xi_2 \tanh(\xi_2 a)\left[\frac{e^2}{\varepsilon^2}\bar{c}'\xi_1' - \frac{e'^2}{\varepsilon'^2}\bar{c}\xi_1 \tan(\xi_1 a)\right]\right\}, \\ M_\Gamma &= \frac{1}{\Gamma}\{\varepsilon\varepsilon'\xi_2 \tanh(\xi_2 a)[\bar{c}\xi_1 \tan(\xi_1 a) - \bar{c}'\xi_1']\}, \\ M_{K\Gamma} &= \frac{\varepsilon\varepsilon'\xi_2 \bar{c}'\xi_1' \tan(\xi_1 a)\bar{c}\xi_1 \tanh(\xi_2 a)}{K\Gamma} \end{aligned} \tag{15}$$

If we consider the electrical imperfection only, i.e., $\Gamma \neq 0$ and $K = \infty$, so $M_K = M_{K\Gamma} = 0$. Eq. (14) can be abbreviated as the form

$$M = M_{\text{perfect}} + M_\Gamma = 0 \tag{16}$$

Similarly, if we consider the mechanical imperfection only, i.e., $K \neq 0$ and $\Gamma = \infty$, so $M_\Gamma = M_{K\Gamma} = 0$. Eq. (14) can be abbreviated as the form

$$M = M_{\text{perfect}} + M_K = 0 \tag{17}$$

which is the outcome by the shear-lag model [22–25]. For the perfect interfaces, i.e., $K = \infty$ and $\Gamma = \infty$, Eq. (14) can be written as

$$M_{\text{perfect}} = 0 \tag{18}$$

which is the same as the work by Yang et al. [9].

4. Numerical results

We choose the trapped mode for consideration, i.e., $\omega_m < \omega < \omega_m'$ [8–10]. The central region and the outer regions are chosen to be PZT-5 and PZT-6B, respectively. The corresponding material parameters are list as Table 1 [27]. As a numerical example, the plate thickness is chosen to be $h = 1$ mm, and $m = 2$.

Contrasting the mechanical imperfection M_K and the electrical imperfection M_Γ in Eq. (15), we can find that M_K has the dominant term of $\bar{c}\xi_1\bar{c}'\xi_1'$ which has order of the product of $\bar{c}$ and $\bar{c}'$, while M_Γ has the dominant term of $(\bar{c}\xi_1 \tan(\xi_1 a) - \bar{c}'\xi')$. Generally speaking, $\bar{c}$ and $\bar{c}'$ have the order of 10^{10} as Table 1 depicted. Hence, if the effective interface elastic stiffness K equals to the electrical imperfection parameter Γ, the value of M_K will be much bigger than that of M_Γ. In order to prove the conclusion, we choose $K = \Gamma = 1 \times 10^{16}$ to calculate M_K and M_Γ. The absolute values of M_K, M_Γ and $M_{K\Gamma}$ are list as Table 2, which shows that the effect of mechanical imperfection is more evident than that of the electrical imperfection.

Table 1
The material parameters.

Materials	ρ (kg/m^3)	c (10^{10} N/m^2)	e (C/m^2)	ε (10^{-8} C/V m)
PZT-6B	7550	3.55	4.6	0.360
PZT-5	7750	2.11	12.3	0.811

Table 2
The absolute values of M_K, M_Γ and $M_{K\Gamma}$.

	The first mode	The third mode	The fifth mode
M_K	1.5415×10^3	1.2136×10^3	0.5618×10^3
M_Γ	5.3950×10^{-18}	5.0565×10^{-18}	4.5370×10^{-18}
$M_{K\Gamma}$	9.4603×10^{-19}	7.2184×10^{-19}	2.9289×10^{-19}

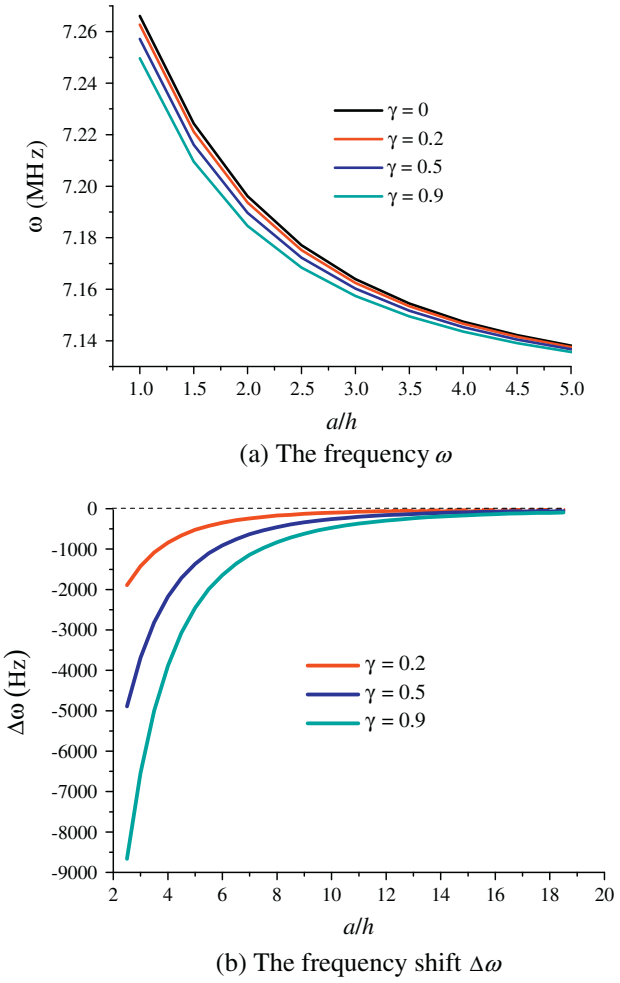

(a) The frequency ω

(b) The frequency shift $\Delta\omega$

Fig. 2. The frequency ω and the frequency shift $\Delta\omega$ of the first mode as a function with the ratio a/h. (a) The frequency ω. (b) The frequency shift $\Delta\omega$.

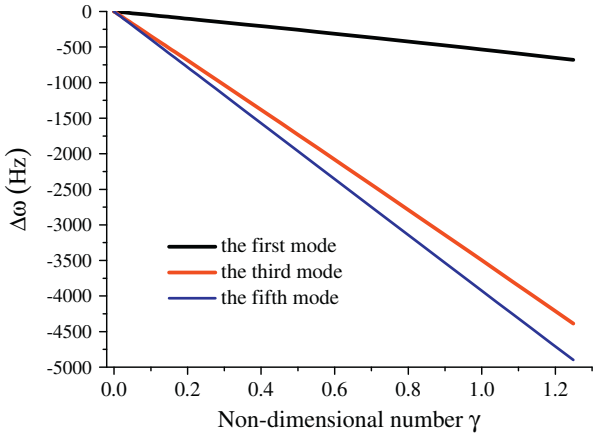

Fig. 3. The frequency change $\Delta\omega$ as a function with γ.

According to Table 2, we only consider the mechanical imperfection in the following, i.e., $\Gamma = \infty$ and $K \neq 0$. Assuming a non-dimensional number $\gamma = \bar{c}\xi_2/K$, so Eq. (14) can be written as the form

$$[\bar{c}'\xi_1' - \bar{c}\xi_1 \tan(\xi_1 a)][\varepsilon' + \varepsilon \tanh(\xi_2 a)] - \xi_2 \varepsilon \varepsilon' \left(\frac{e}{\varepsilon} - \frac{e'}{\varepsilon'}\right)^2 \tanh(\xi_2 a) = \gamma \left\{ \frac{\xi_1 \bar{c}' \xi_1' \tan(\xi_1 a)}{\xi_2} [\varepsilon' + \varepsilon \tanh(\xi_2 a)] + \frac{\varepsilon \varepsilon' \tanh(\xi_2 a)}{\bar{c}} \left[\frac{e^2}{\varepsilon^2} \bar{c}' \xi_1' - \frac{e'^2}{\varepsilon'^2} \bar{c} \xi_1 \tan(\xi_1 a) \right] \right\} \quad (19)$$

where $\gamma = 0$, i.e., $K = \infty$ is related to the perfect interfaces. The frequency shift can be defined as $\Delta\omega = \bar{\omega} - \omega_0$, where $\bar{\omega}$ is the frequency of the plate when the interfaces are imperfect, and ω_0 represents the frequency of the plate with the perfect interfaces. Fig. 2 is the frequency ω and the frequency shift $\Delta\omega$ of the first mode as the function with the ratio a/h.

Owning to the relation $\omega_m < \omega_m'$, the frequency of the first mode decreases with the increasing a/h, this can be seen from Fig. 2a. On the other hand, the frequencies will decrease if the interfaces are imperfectly bonded, which is because the imperfect interfaces reduce the stiffness of the plate. The two points illustrate the validity of the phase velocity equations obtained in our research work. When the ratio a/h is small, the imperfect interfaces make a great impact on the frequencies of the plate, and with the ratio a/h increasing, this kind of effect falls off, which can be seen from Fig. 2b. The frequencies of the higher modes have the

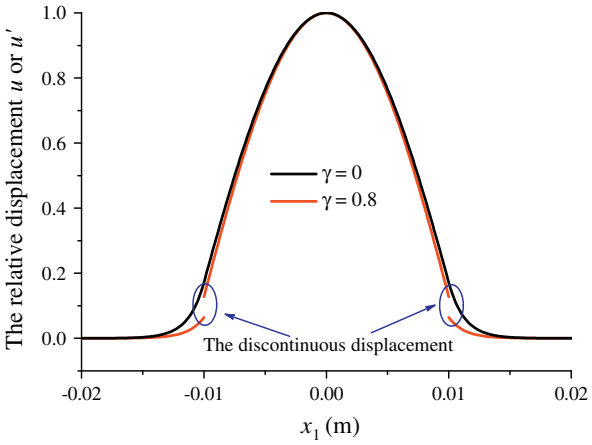

Fig. 4. The relative displacement of the first mode along the x_1 direction when $A_1 = 1$ and $\omega = 7.122$ MPa.

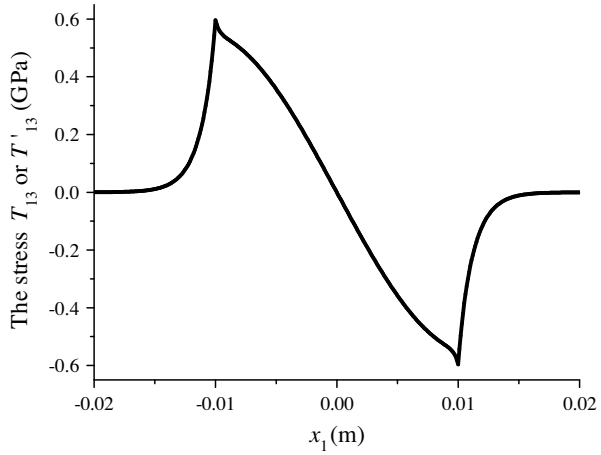

(a) The stress component of the imperfectly bonded plate

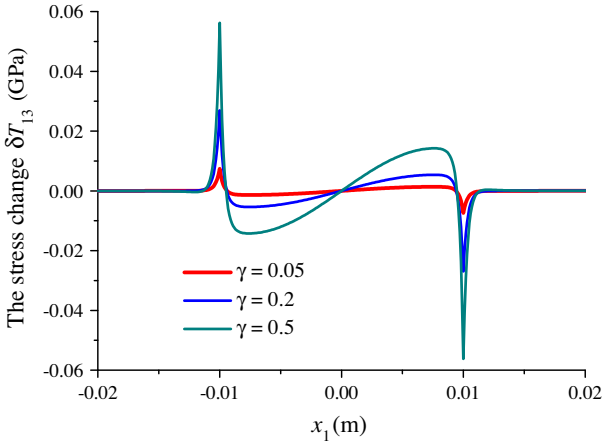

(b) The stress change δT_{13}

Fig. 5. The stress component and the stress change δT_{13} of the first mode along the x_1 direction when $A_1 = 10^{-4}$ and $\omega = 7.122$ MPa.

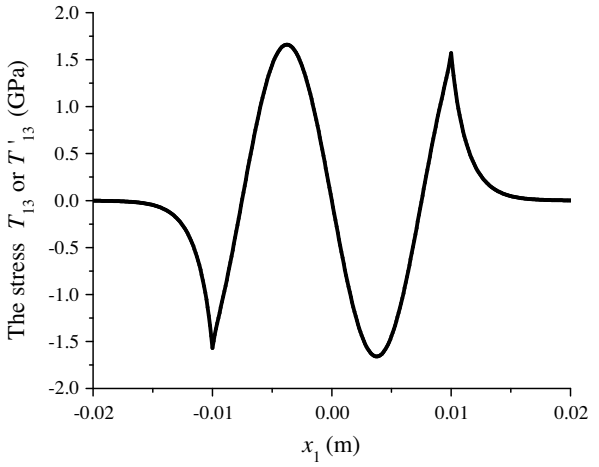

(a) The stress component of the imperfectly bonded plate

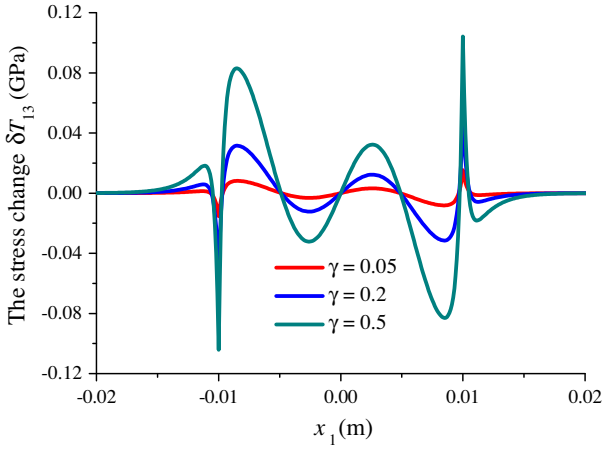

(b) The stress change δT_{13}

Fig. 6. The stress component and the stress change δT_{13} of the third mode along the x_1 direction when $A_1 = 10^{-4}$ and $\omega = 7.178$ MPa.

same tendency with the increasing ratio a/h, which are not depicted here. In the following discussion, we choose $a/h = 10$.

Fig. 3 is the frequency shift $\Delta\omega$ as a function with γ. From Fig. 3, we can conclude that the frequency shift $\Delta\omega = 0$ if the interfaces are perfect, i.e., $\gamma = 0$ or $K = \infty$, which also provides that our computation results are correct. Compared with the higher order modes, the first mode has a relatively smaller frequency change. The relationship between the frequency shift $\Delta\omega$ and the non-dimensional number γ is linear, which can be explained by Chen et al. [24]. This relationship can be used to provide the foundation for a new experimental procedure for measuring the level of the interface bonding.

In order to deal with the imperfect interface, the spring-type relation can be applied, in which the interface can be treated as a layer that geometrically has a zero thickness but the tangential displacement is allowed to be different from both sides of the interface, so the discontinuous displacement can be seen at the imperfect interfaces, which can be proved by Fig. 4. Whether the interface is imperfect or not, the amplitude of the displacement component decays rapidly along the x_1 direction when the frequency of the plate ω satisfies $\omega_m < \omega < \omega'_m$. In the region $|x_1| > 0.02$ m, the displacement almost equals to zero, which means we cannot receive the thickness–twist waves. This is related to the energy-trapping phenomenon of the thickness–twist modes [7–11], in which the vibration is confined to the central portion of the plate and essentially, there is almost no vibration in the rest of the plate. So the plate can meet practical needs, such as wiring and mounting, in which the vibration of the outer portion cannot affect the central portion. On the other hand, the displacement in the case of imperfectly bonding is a little bit smaller than that in the case of perfectly bonding because the imperfectly bonding also absorbs some energy of the waves when they propagate through it. The displacement components of the higher modes have the similar tendency along the x_1 direction, which are not discussed here.

Similar with $\Delta\omega$, we can also define δT_{13} as the stress change. Figs. 5–7 are the stress component T_{13} or T'_{13} and the stress change δT_{13} along the x_1 direction when $A_1 = 10^{-4}$. The energy-trapping phenomenon of the thickness–twist modes also can be seen owning to the frequency ω we adopted satisfies $\omega_m < \omega < \omega'_m$, and the stress component T_{13} or T'_{13} and the stress change δT_{13} are all antisymmetric about $x_1 = 0$, which is because of the symmetric mode of the displacement component and the electrical potential function we adopted in Eqs. (9) and (11). Considering the imperfect interfaces, the stress component changes more evidently in the central portion $x_1 < |a|$ than in the outer portions $x_1 > |a|$, especially the stress T_{13} or T'_{13} changes most severely at the imperfect interfaces, which can be seen from Figs. 5–7.

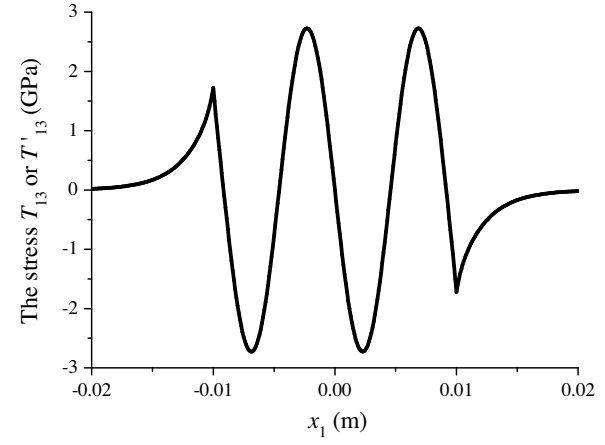

(a) The stress component of the imperfectly bonded plate

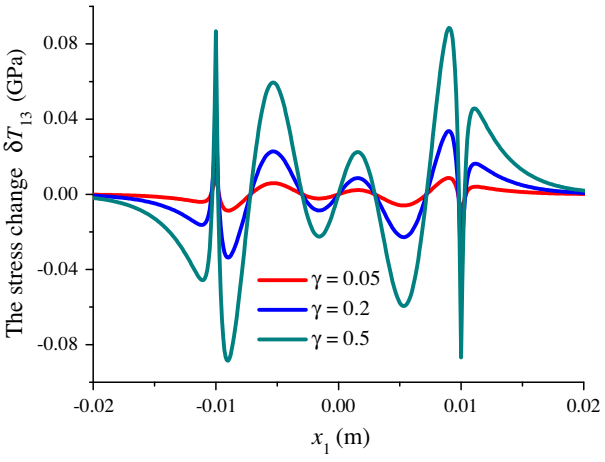

(b) The stress change δT_{13}

Fig. 7. The stress component and the stress change δT_{13} of the fifth mode along the x_1 direction when $A_1 = 10^{-4}$ and $\omega = 7.283$ MPa.

5. Conclusions

The effect of the imperfectly bonded interfaces about the thickness–twist mode in an inhomogeneous piezoelectric plate in which the central portion is different from the rest portions is analyzed with the spring-type relation, which simultaneously takes the mechanical imperfection and the electrical imperfection into account. Results show that the effect of mechanical imperfection is more evident than that of the electrical imperfection. The linear relationship between the frequency shift $\Delta\omega$ and the non-dimensional number γ can be used to measure the level of the interface bonding. The results theoretically can be used in the design of wave propagation in the piezoelectric coupled structures with an imperfect interface.

Acknowledgments

The financial support of the work by the National Natural Science Foundation of China (No. 10972171), the Program for New Century Excellent Talents in Universities (No. NCET–08–0429) and the National 111 Project of China (No. B06024) are gratefully acknowledged.

References

[1] J.F. Tressler, S. Alkoy, A. Dogan, R.E. Newnham, Functional composites for sensors, actuators and transducers, Composites Part A: Applied Science and Manufacturing 30 (1999) 477–482.
[2] H.F. Tiersten, Wave propagation in an infinite piezoelectric plate, The Journal of the Acoustical Society of America 35 (1963) 234–239.
[3] B. Jakoby, M.J. Vellekoop, Properties of Love waves: applications in sensors, Smart Materials and Structures 6 (1997) 668–679.
[4] J.L. Bleustein, A new surface wave in piezoelectric material, Applied Physics Letters 13 (1968) 412–413.
[5] R.D. Mindlin, Bechmann's number for harmonic overtones of thickness/twist vibrations of rotated Y-cut quartz plates, The Journal of the Acoustical Society of America 41 (1967) 969–973.
[6] G.T. Pearman, Thickness–twist vibrations in beveled AT-cut quartz plates, The Journal of the Acoustical Society of America 45 (1969) 928–934.
[7] J.L. Bleustein, Some simple modes of wave propagation in an infinite piezoelectric plate, The Journal of the Acoustical Society of America 45 (1969) 614–620.
[8] J.L. Bleustein, Thickness–twist and face–shear vibrations of a contoured crystal plate, International Journal of Solids and Structures 2 (1966) 351–360.
[9] J. Yang, Z. Chen, Y. Hu, Trapped thickness–twist modes in an inhomogeneous piezoelectric plate, Philosophical Magazine Letters 86 (2006) 699–705.

[10] J. Yang, Z. Chen, Y. Hu, Propagation of thickness–twist waves through a joint between two semi-infinite piezoelectric plates, IEEE Transactions on Ultrasonics, Ferroelectrics and Frequency Control 54 (2007) 888–891.
[11] J. Yang, Z. Chen, Y. Hu, S. Jiang, S. Guo, Propagation of thickness–twist waves in a multi-sectioned piezoelectric plate of 6 mm crystals, Archive of Applied Mechanics 77 (2007) 689–696.
[12] F. Jin, Z. Wang, T. Wang, The Bleustein–Gulyaev (B–G) wave in a piezoelectric layered half-space, International Journal of Engineering Science 39 (2001) 1271–1285.
[13] Q. Wang, V.K. Varadan, Wave propagation in piezoelectric coupled plates by use of interdigital transducer: Part 1. Dispersion characteristics, International Journal of Solids and Structures 39 (2002) 1119–1130.
[14] J. Liu, Z.K. Wang, The propagation behavior of Love waves in a functionally graded layered piezoelectric structure, Smart Materials and Structures 14 (2005) 137–146.
[15] Z. Qian, F. Jin, Z. Wang, K. Kishimoto, Transverse surface waves on a piezoelectric material carrying a functionally graded layer of finite thickness, International Journal of Engineering Science 45 (2007) 455–466.
[16] H. Liu, Z.B. Kuang, Z.M. Cai, Propagation of Bleustein–Gulyaev waves in a prestressed layered piezoelectric structure, Ultrasonics 41 (2003) 397–405.
[17] Z. Qian, F. Jin, Z. Wang, K. Kishimoto, Love waves propagation in a piezoelectric layered structure with initial stresses, Acta Mechanica 171 (2004) 41–57.
[18] Z. Qian, F. Jin, K. Kishimoto, Z. Wang, Effect of initial stress on the propagation behavior of SH-waves in multilayered piezoelectric composite structures, Sensors and Actuators A: Physical 112 (2004) 368–375.
[19] F.L. Guo, R. Sun, Propagation of Bleustein–Gulyaev wave in 6 mm piezoelectric materials loaded with viscous liquid, International Journal of Solids and Structures 45 (2008) 3699–3710.
[20] P. Kielczynski, R. Plowiec, Determination of the shear impedance of viscoelastic liquids using Love and Bleustein–Gulyaev surface waves, The Journal of the Acoustical Society of America 86 (1989) 818–827.
[21] J.R. Vig, A. Ballato, Comments on the effects of nonuniform mass loading on a quartz crystal microbalance, IEEE Transactions on Ultrasonics, Ferroelectrics and Frequency Control 45 (1998) 1123–1124.
[22] Y. Huang, X.F. Li, K.Y. Lee, Interfacial shear horizontal (SH) waves propagating in a two-phase piezoelectric/piezomagnetic structure with an imperfect interface, Philosophical Magazine Letters 89 (2009) 95–103.
[23] Y. Huang, X.F. Li, Shear waves guided by the imperfect interface of two magnetoelectric materials, Ultrasonics 50 (2010) 750–757.
[24] J. Chen, W. Wang, J. Wang, Z. Yang, J. Yang, A thickness mode acoustic wave sensor for measuring interface stiffness between two elastic materials, IEEE Transactions on Ultrasonics, Ferroelectrics and Frequency Control 55 (2008) 1678–1681.
[25] F. Jin, K. Kishimoto, H. Qing, Hisahiro Inoue, T. Tateno, Influence of imperfect interface on the propagation of Love waves in piezoelectric layered structures, Key Engineering Materials 26 (2004) 251–256.
[26] Y. Li, K. Yong Lee, Effect of an imperfect interface on the SH wave propagating in a cylindrical piezoelectric sensor, Ultrasonics 50 (2010) 473–478.
[27] S.N. Jiang, Q. Jiang, X.F. Li, S.H. Guo, H.G. Zhou, J.S. Yang, Piezoelectromagnetic waves in a ceramic plate between two ceramic half-spaces, International Journal of Solids and Structures 43 (2006) 5799–5810.